International Journal of Applied Mathematics and Engineering Sciences
Vol. 3 No. 1 (January-June, 2018)

A SIX DEGREES OF FREEDOM TRAJECTORY SIMULATION ANALYSIS FOR PROJECTILES AND SMALL BULLETS

Dimitrios N. Gkritzapis, Elias E. Panagiotopoulos
Dionissios P. Margaris & Dimitrios G. Papanikas

Received: 03rd March 2017 Revised: 14th April 2017 Accepted: 10th September 2017

ABSTRACT: A full six degrees of freedom (6-DOF) flight dynamics model is applied for the accurate prediction of short and long-range trajectories of high spin-stabilized projectiles and small bullets via atmospheric flight to final impact point. The mathematical model is based on the full equations of motion set up in the no-roll body fixed reference frame and is integrated numerically from given initial conditions at the firing site. The projectile maneuvering motion depends on the most significant force and moment variations, in addition to crosswind, gravity and Magnus effect. The computational flight analysis takes into consideration the Mach number and total angle of attack effects by means of the variable aerodynamic coefficients. For the purposes of the present work, linear interpolation has been applied for aerodynamic coefficients from the official tabulated database. The developed computational method gives satisfactory agreement with published data of verified experiments and computational codes on atmospheric projectile trajectory analysis for various initial firing flight conditions.

1. INTRODUCTION

Ballistics is the science that deals with the motion of projectiles. The word ballistics was derived from the Latin "ballista", which was an ancient machine designed to hurl a javelin. The modern science of exterior ballistics[1] has evolved as a specialized branch of the dynamics of rigid bodies, moving under the influence of gravitational and aerodynamic forces and moments. Exterior ballistics existed for centuries as an art before its first beginnings as a science. Although a number of sixteenth and seventeenth century European investigators contributed to the growing body of renaissance knowledge, Isaac Newton of England (1642-1727) was probably the greatest of the modern founders of exterior ballistics. Newton's laws of motion established, without which ballistics could not have advanced from an art to a science.

Pioneering English ballisticians Fowler, Gallop, Lock and Richmond[2] constructed the first rigid six-degree-of-freedom projectile exterior ballistic model. Various authors has extended this projectile model for lateral force impulses[3,4] , linear theory in atmospheric flight for dual-spin projectiles[5,6], aerodynamic jump extending analysis due to lateral impulsives[7] and aerodynamic asymmetry[8], instability of controlled projectiles in ascending or descending flight[9]. Costello's modified linear theory[10] has also applied recently for rapid trajectory projectile prediction.

The present work address a full six degrees of freedom (6-DOF) projectile flight dynamics analysis to be applied for the accurate prediction of short and long range trajectories of high spin-stabilized projectiles and small bullets. The applied aerodynamic coefficient analysis takes into consideration the influence of the most significant force and moment variations, depending on the Mach number flight and total angle of attack. The computational simulation of the applied variable flight model gives results of high accuracy in contrast to a corresponding analysis with constant aerodynamic coefficients.

The efficiency of the developed method gives satisfactory results compared with published data of verified experiments and computational codes on dynamics model analysis of short and long-range trajectories of spin-stabilized projectiles and small bullets.

2. TRAJECTORY FLIGHT SIMULATION MODEL

A six degree of freedom rigid-projectile model[11,12,13,14] has been employed in order to predict the "free" atmospheric trajectory to final target area without any control practices. The six degree of freedom flight analysis comprises the three translation components (x, y, z) describing the position of the projectile's center of mass and three Euler angles (φ, θ, ψ) describing the orientation of the projectile body with respect to Fig.1.

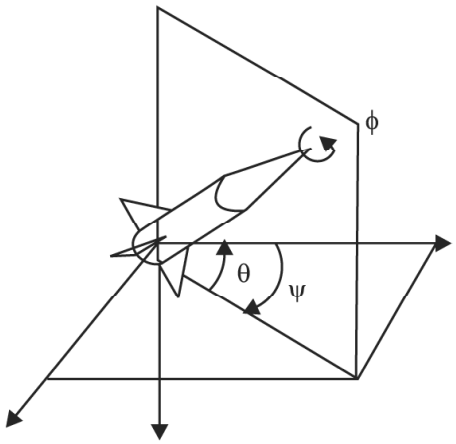

Figure 1: Projectile Orientation Definitions (Euler Angles)

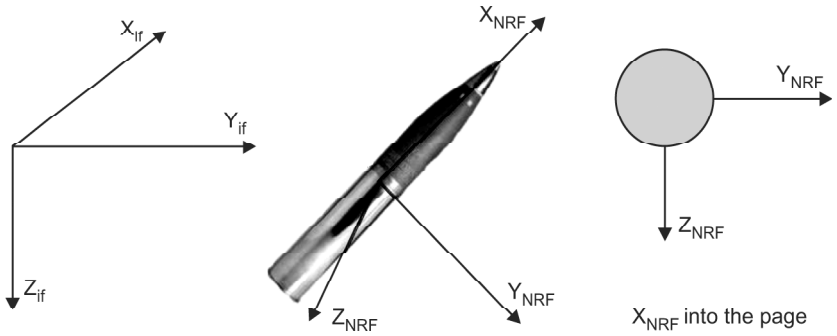

Figure 2: No-roll (moving) and Fixed (inertial) Coordinate Systems for the Projectile Trajectory Analysis

Two main coordinate systems (Fig. 2) are used for the computational approach of the atmospheric flight motion. The one is an Earth-fixed coordinate system (inertial frame, IF) which the X_{IF}–Y_{IF} plane is tangent to the Earth's' surface at the launch point, and X_{IF} axis points downrange. The Z_{IF} axis points vertically downward through the launch point and the Y_{IF} axis points to the right, when looking downrange. The other is a no-roll rotating coordinate system that is attached to, and moving with, the projectile's center of mass (no-roll-frame, NRF, φ = 0) with X_{NRF} axis along the projectile's axis of rotational symmetry positive from tail to nose. Y_{NRF} axis is perpendicular to X_{NRF} lying in the horizontally plane and Z_{NRF} axis oriented to complete a right-hand orthogonal system.

Newton's laws of the motion state that the rate of change of linear momentum must equal the sum of all the externally applied forces and the rate of change of angular momentum must equal the sum of the externally applied moments, as shown respectively in the following forms:

$$m\frac{d\vec{V}}{dt} = \vec{F}_{tot}, \frac{d\vec{H}}{dt} = \vec{M}_{tot}$$

Therefore, the twelve state variables x, y, z, φ, θ, ψ, u, v, w, p, q and r are necessary to describe position, flight direction and velocity at every point of the projectile's atmospheric flight trajectory. Introducing the components of the acting forces and moments expressed in the no-roll-frame (~) rotating coordinate system in Eqs (1, 2) with the dimensionless arc length s as an independent variable measured in calibers of travel, the following full equations of motion are derived:

$$x' = \frac{D}{V}\cos\psi \ \cos\theta \ \tilde{u} - \frac{D}{V} \ \sin\psi \ \tilde{v} + \tilde{w} \ \cos\psi \ \sin\theta \ \frac{D}{V} \tag{3}$$

$$y' = \frac{D}{V} \ \cos\theta \ \sin\psi \ \tilde{u} + \tilde{v}\cos\psi \ \frac{D}{V} + \tilde{w} \ \sin\theta \sin\psi \frac{D}{V} \tag{4}$$

$$z' = -\frac{D}{V} \ \sin\theta \ \tilde{u} + \frac{D}{V} \ \tilde{w}\cos\theta \tag{5}$$

$$\phi' = \frac{D}{V}\tilde{p} + \frac{D}{V} \ \tan\theta \ \tilde{r} \qquad \theta' = \frac{D}{V} \ \tilde{q} \qquad \psi' = \frac{D}{V\cos\theta} \ \tilde{r} \tag{6, 7, 8}$$

$$\tilde{u}' = -\frac{D}{V}g\sin\theta - K_1 V C_D - K_1 V C_D^2 \alpha^2 - K_1 V C_D^2 \beta^2 + \tilde{v}\frac{D}{V}\tilde{r} - \tilde{q}\frac{D}{V}\tilde{w} \tag{9}$$

$$\tilde{v}' = -K_1 \ \left(C_D + C_L\right) \ \left(\tilde{v} - \tilde{v}_w\right) + D\frac{K_1}{2}\tilde{p} \ C_{MaF} \ \alpha - \frac{D}{V}\tilde{r} \ \tilde{w}\tan\theta - \frac{D}{V}\tilde{r} \ \tilde{u} \tag{10}$$

$$\tilde{w}' = \frac{D}{V}g \ \cos\theta - K_1 \ \left(C_D + C_L\right) \ \left(\tilde{w} - \tilde{w}_w\right) - D \ \frac{K_1}{2}\tilde{p} \ C_{MaF} \ \beta + \frac{D}{V} \ \tilde{q} \ \tilde{u} + \ \tan\theta\frac{D}{V}\tilde{r} \ \tilde{v} \tag{11}$$

$$\tilde{p}' = D^5 \frac{\pi}{16 I_{XX}} \tilde{p}\rho C_{RD} \tag{12}$$

$$\begin{aligned}\tilde{q}' = {} & 2K_2\left(C_D + C_L\right) \ \left(\tilde{w} - \tilde{w}_w\right) \ L_{CGCP} + D\frac{K_2}{V} \ C_{MaM}\tilde{p}\left(\tilde{v} - \tilde{v}_w\right)L_{CGCM} + \\ & + D^2 K_2 \ C_{PD} \ \tilde{q} + D \ 2K_2 C_{OM} \ -\frac{D}{V}\tilde{r} \ \frac{I_{XX}}{I_{YY}}\tilde{p} - \frac{D}{V}\tilde{r}^2\tan\theta\end{aligned} \tag{13}$$

$$\begin{aligned}\tilde{r}' = {} & -2K_2\left(C_D + C_L\right)\left(\tilde{v} - \tilde{v}_w\right) \ L_{CGCP} + \ D \ \frac{K_2}{V}\tilde{p} \ C_{MaM}\left(\tilde{w} - \tilde{w}_w\right)L_{CGCM} + \\ & + D^2 K_2 C_{PD}\tilde{r} - 2 \ DK_2 C_{OM} \ + \frac{D}{V} \ \tilde{p} \ \tilde{q}\frac{I_{XX}}{I_{YY}} + \frac{D}{V} \ \tilde{q}\tilde{r}\tan\theta\end{aligned} \tag{14}$$

The projectile dynamics trajectory model consists of twelve non-linear first order ordinary differential equations, which are solved simultaneously by resorting to numerical integration using a 4th order Runge-Kutta method.

Modified linear theory makes several assumptions regarding the relative size of different quantities to further simplify the analysis: the Euler angle ψ is small so $\sin\psi \approx \psi$, $\cos\psi \approx 1$. The axial velocity $\tilde{u}$ replaced by the total velocity V because the side velocities $\tilde{v}$ and $\tilde{w}$ are small. The aerodynamic angles of attack α and sideslip β are small for the main part of the atmospheric trajectory $\alpha \approx \tilde{w}/V, \beta \approx \tilde{v}/V$. The projectile is mass-balanced such that $I_{XY} = I_{YZ} = I_{XZ} = 0$, $I_{YY} = I_{ZZ}$.

Quantities V and φ are large compared to ϕ, $\tilde{q}$, $\tilde{r}$, and , such that products of small quantities and their derivatives are negligible. In projectile linear theory, the Magnus forces in equations 10, 11 typically regarded as small and dropped. Magnus moments due to the fact that a cross product between Magnus force and its respective moment arm is not necessarily small.

With the aforementioned assumptions, the above expressions results in:

$$x' = D\cos\theta \tag{3i}$$

$$y' = D\cos\theta\psi \tag{4i}$$

$$z' = D\sin\theta \tag{5i}$$

$$V' - \frac{D}{V}g \quad \sin\theta - K_1 V C_D \tag{9i}$$

$$\tilde{v}' = -K_1 \quad \left(C_D + C_{La}\right)\left(\tilde{v} - \tilde{v}_w\right) - D\tilde{r} \tag{10i}$$

$$\tilde{w}' = \frac{D}{V}g \quad \cos\theta - K_1\left(C_D + C_{La}\right)\left(\tilde{w} - \tilde{w}_w\right) + D\tilde{q} \tag{11i}$$

$$\tilde{q}' = 2K_2\left(C_D + C_{La}\right) \quad \left(\tilde{w} - \tilde{w}_w\right)L_{CGCP} + D \quad \frac{K_2}{V} \quad C_{MaM} \quad \tilde{p} \quad \left(\tilde{v} - \tilde{v}_w\right)L_{CGCM} + \\ + D^2 K_2 C_{PD}\tilde{q} + 2D \quad K_2 C_{OM} \tag{13i}$$

$$\tilde{r}' = -2K_2\left(C_D + C_{La}\right)\left(\tilde{v} - \tilde{v}_w\right)L_{CGCP} + D\frac{K_2}{V}\tilde{p}C_{MaM}\left(\tilde{w} - \tilde{w}_w\right)L_{CGCM} + D^2 K_2 C_{PD}\tilde{r} - 2DK_2 C_{OM} \tag{14i}$$

The equations 6, 7, 8 and 12 remain invariable.

A constant dynamic flight model[15] with mean values of the experimental average aerodynamic coefficients variations[1] gives a first estimation of the atmospheric trajectory motion. Moreover, during the atmospheric flight of the projectile or bullet there is an important change of the angle of attack and the Mach number. Therefore, it is more convenient to use variable aerodynamic coefficients for the accurate computational simulation of free-flight projectile and bullet motion in order to predict the final target shooting area. For this purpose, linear interpolation for variable coefficients has been applied, taking from official tabulated exterior ballistics database[1].

3. ATMOSPHERIC MODEL

Atmospheric properties of air, like density ρ, are being calculated based on a standard atmosphere from the International Civil Aviation Organization (ICAO).

4. PROJECTILE MODEL

The present analysis considers two different types of representative projectiles. A typical formation of the cartridge 105mm HE M1 projectile is presented in Fig. 3, and is used with various 105mm howitzers such as M49 with M52, M52A1 cannons, M2A1 & M2A2 with M101, M101A1 cannons, M103 with M108 cannon, M137 with M102 cannon as well as NATO L14 MOD56 and L5. Cartridge 105 mm HE M1 is of semi-fixed type ammunition, using adjustable propelling charges in order to achieve desirable ranges. The projectile producing both fragmentation and blast effects can be use against personnel and materials targets.

Also a 0.30 caliber (0.308" diameter), 168 grain (≈ 10.9 gr) Sierra International bullet used by National Match M14 rifle is loaded into 7.62 mm M852 match ammunition for high power rifle competition shooting, as shown in Fig. 4. The cartridge is intended and specifically prepared for used in those weapons designed as competitive rifles and for marksmanship training. This bullet is not for combat use. The cartridge case head stamping of MATCH identify the cartridge. It also has a knurl at the base of the cartridge case and a hollow point boat-tail bullet.

Basic physical and geometrical characteristics data of the above-mentioned 105 mm HE M1 projectile and 7.62 mm bullet illustrated briefly in Table 1.

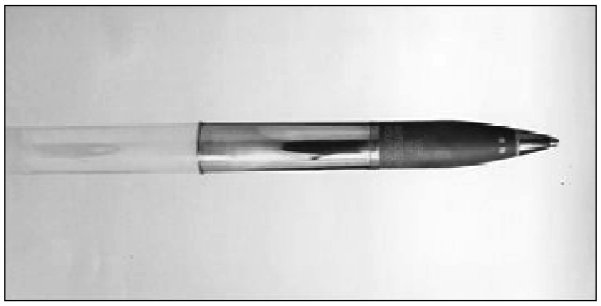

Figure 3: 105 mm HE M1 High Explosive Projectile Artillery Ammunition for howitzers.

Figure 4: 7.62 mm Match Ammunition with a Diameter of 0.30 Caliber Representative Small Bullet Types

Table 1
Physical and Geometrical Data of 105 mm big Projectile and 7.62 mm Small Bullet Types

Characteristics	*105 mm HE M1 projectile*	*7.62 mm M852 bullet*
Reference diameter, mm	104.8	7.62
Total length, mm	494.7	71.88
Total mass, kg	15.00	0.385
Axial moment of inertia, kg·m^2	$2.326 \cdot 10^{-2}$	$7.2282 \cdot 10^{-8}$
Transverse moment of inertia, kg·m^2	$2.3118 \cdot 10^{-1}$	$5.3787 \cdot 10^{-7}$
Center of gravity from the base, mm	183.4	12.03

In our present analysis, we will assume that the yaw level is small enough to neglect geometric nonlinearity, but will retain all significant aerodynamic forces and moments.

5. GYROSCOPIC STABILITY

Any spinning object will have gyroscopic properties. Classical exterior ballistics[1] defines the gyroscopic stability factor S_g in the following generalized form:

$$S_g = \frac{I_{XX}^2 \tilde{p}^2}{2\rho I_{YY} S_{ref} D V^2 C_{OM}} \tag{15}$$

This may be rearranged into:

$$S_g = \left(\frac{2I_{XX}^2}{I_{YY}\pi D^3}\right)\left(\frac{\tilde{p}}{V}\right)^2\left(\frac{1}{C_{OM}}\right)\left(\frac{1}{\rho}\right) \tag{16}$$

The aforementioned Eq. (16) shows that the static factor is proportional to four terms product, depending on the geometric technical characteristics of the projectile shape model, the square axial spin to velocity ratio, the aerodynamic overturning moment coefficient C_{OM} and the atmospheric density variation ρ.

6. INITIAL SPIN RATE ESTIMATION

In order to have a statically stable flight projectile trajectory motion, the initial spin rate $\tilde{p}_0$ prediction at the gun muzzle in the firing site is important. According to McCoy definitions[1], the following form is used:

$$\tilde{p}_0 = 2\pi V_0 / \eta D \quad (rad/s) \tag{17}$$

where V_0 is the initial axial firing velocity (m/s), η the rifling twist rate at the gun muzzle (calibers per turn), and D the reference diameter of the projectile type (m). Typical values of rifling twist η are 1/18 calibers per turn for big projectile and 12 inches per turn for small bullet, respectively.

7. COMPUTATIONAL SIMULATION

The flight dynamic model applied on 105 mm HE M1 and 7.62 mm projectile types involves the solution of the set of the twelve nonlinear first order ordinary differentials, Eqs (3-14). It is solved simultaneously by resorting to numerical integration using a 4th order Runge-Kutta method, and regard to the 6-D nominal non-thrusting and non-constrained atmospheric projectile flight.

Initial flight conditions for both dynamic flight simulation models with constant and variable aerodynamic coefficients illustrated in Table 2 for the examined test cases.

Table 2
Initial Flight Parameters of the Projectile Examined Test Cases

Initial Flight Data	*105 mm HE M1 Projectile*	*7.62 mm bullet*
x, m	0.0	0.0
y, m	0.0	0.0
z, m	0.0	0.0
φ, deg	0.0	0.0
θ, deg	15°, 30°, 45°, 60°and 70°	0.84°, 10°, 20° and 32°
ψ, deg	3.0	2.0
u, m/s	494.0	792.48
v, m/s	0.0	0.0
w, m/s	0.0	0.0
p, rad/s	1,644.0	16,335.0
q, rad/s	0.0	0.0
r, rad/s	3.61 and 3.64	25.0

8. RESULTS AND DISCUSSION

The flight path trajectory motions with constant aerodynamic coefficients of the big 105 mm projectile with initial firing velocity of 494 m/sec, initial yaw angle 3 degrees, rifling twist rate 1 turn in 18 calibers (1/18) and initial yaw rates 3.61 rad/s and 3.64 rad/s at 45° and 70°, respectively, are indicated in Fig. 5.

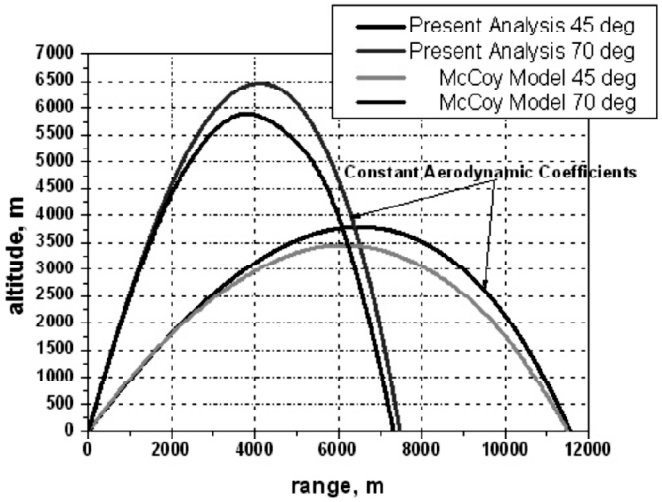

Figure 5: Impact Points and Flight Path Trajectories with Constant Aerodynamic Coefficients for 105 mm Projectile Compared with McCoy's Trajectory Data

The calculated impact points of the above no-wind trajectories with the proposed constant aerodynamic coefficients compared with accurately estimations of McCoy's flight trajectory analysis[1] provide basic differences for the main part of the atmospheric flight motion for the same initial flight conditions.

On the other hand in Fig. 6, the present study of the 105 mm HE M1 projectile trajectory motion with variable aerodynamic coefficients compared with McCoy's flight atmospheric model at pitch angles of 45° and 70°, provide satisfactory agreement for the same conditions. The diagram shows that the predicted range to impact for 105 mm HE M1 projectile, fired at sea-level with an angle of 45° (cyan solid line) and no wind, is 11,500 m and the maximum height is 3,490 m. At 70° (green solid line), the predicted shooting point is 7,310 m, and the maximum height is slight over 6,000 m. The flight path trajectories with initial pitch angles of 15°, 30° and 60° are also shown in the same figure in comparison with the 45° and 70° flight motions. It can be stated that the maximum impact range is at 45° initial firing angle while the minimum presents at 15°.

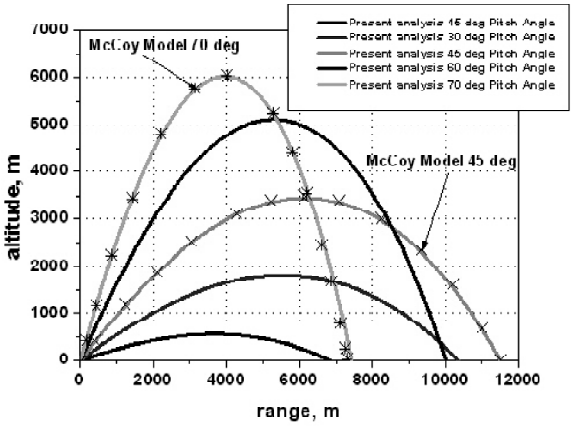

Figure 6: Impact Points and Flight Path Trajectories with Variable Aerodynamic Coefficients for 105 mm Projectile at Low and High Quadrant Elevation Angles of 15°, 30°, 45°, 60° and 70° Compared with McCoy's Trajectory Data

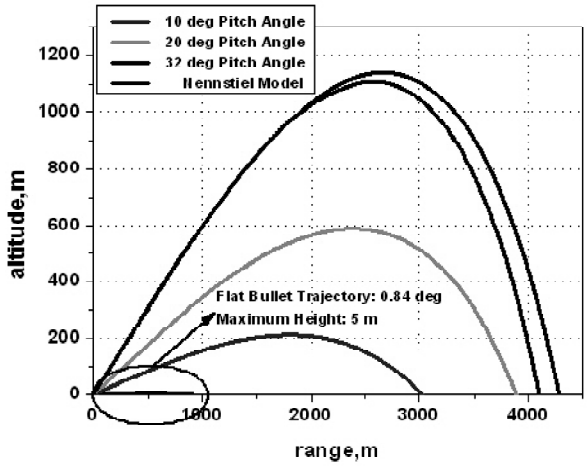

Figure 7: Altitude-Range Maps with Variable Aerodynamic Coefficients Applied on 7.62 mm Bullet at Quadrant Elevation Angles of 0.84°, 10°, 20° and 32° Compared with Nennstiel's Model Trajectory

The small bullet of 7.62 mm diameter is also examined for its atmospheric variable flight trajectories predictions in Fig. 7 at low and high pitch angles of 0.84°, 10°, 20°, 32°, with initial firing velocity of 793 m/s, initial yaw angle 2°, yaw rate 25 rad/s and rifling twist 12 inches per turn. The impact points of the above trajectories are compared with an accurately flight path prediction with Nennstiel's trajectory analysis[16] for cartridge 7.62 mm ball M80 bullet type with initial firing velocity of 838 m/s. At 0.84°, the 7.62 mm M852 bullet, fired at no wind sea-level conditions gives a range to impact at 920 m with a maximum height at almost 5 m. At 32°, the predicted level-ground range is approximately 4,280 m and the height is 1,140 m. For the same initial pitch angle, the 7.62 mm M80 ball-bullet of Nennstiel's flight path has a smaller range to impact and a maximum height at 1,170 m.

Variations of velocity are investigated in Fig. 8 for the 105 mm HE M1 projectile trajectory motion firing at 494m/sec with variable aerodynamic coefficients at pitch angles of 45° and 70°. It is obvious that at 45°, the velocity drops to the value of 230 m/sec at the maximum height and then grows to the final value of almost 300 m/sec at the impact target shooting area. Furthermore, at 70° the minimum velocity reaches the value of 100 m/sec at about 4000 m downward range, whereas the final flight velocity is almost 340 m/sec.

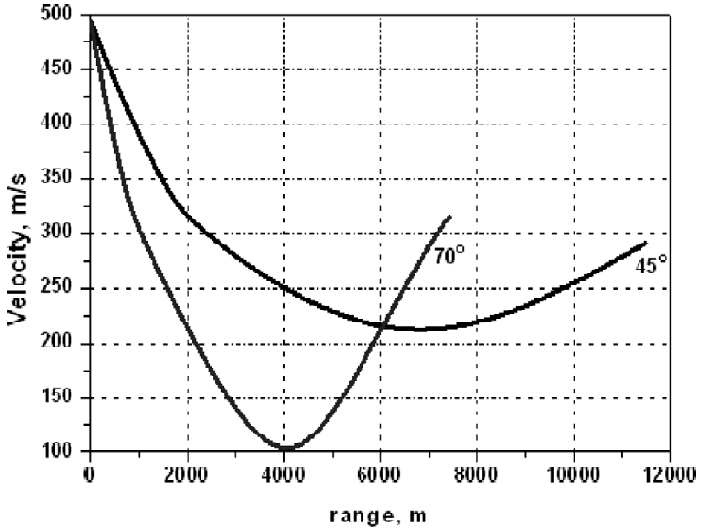

Figure 8: Velocity-Range Curves for the 105 mm Big Projectile Atmospheric Motion with Variable Aerodynamic Coefficients at Elevation Angles of 45° and 70°

On the other hand, the same curves for the flight velocity change are also calculated in the case of the small 7.62 mm bullet (Fig. 9) with an initial launching velocity 793 m/sec at pitch angles of 10 and 32 degrees. The computational results give the final values of 150 and 140 m/sec, respectively, at the impact target area.

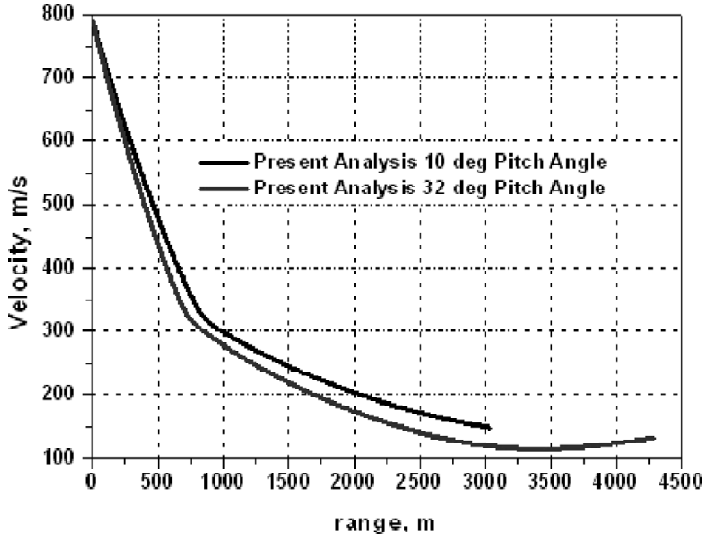

Figure 9: Variable Flight Model to Impact Target Point Applied on 7.62 mm Bullet at Elevation Angles of 10° and 32°

In addition, Fig. 10 shows that the total times of flight for the 105 mm HE M1 projectile variable atmospheric motion, fired at sea-level neglecting wind conditions, at pitch angles of 45° and 70° are almost 53 and 73 sec, respectively. Furthermore, the same indicated in Fig. 11 for the 7.62 mm bullet at pitch angles of 10° and 32°, where the corresponding times to final impact point is 12 and 27 sec, respectively. The above results state that, the time of projectile flight motion is short so the applied variable rapid trajectory prediction is taken into account for high accuracy impact target shooting.

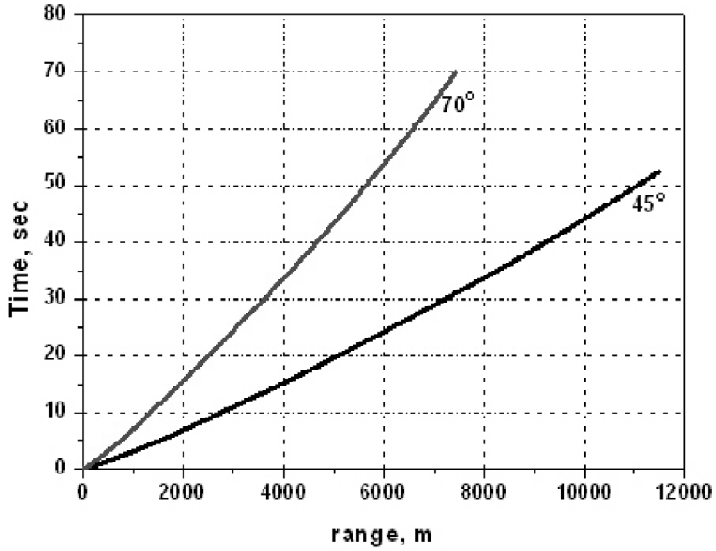

Figure 10: Times of Atmospheric Flight for 105 mm big Projectile at Pitch Angles of 45° and 70°, Respectively

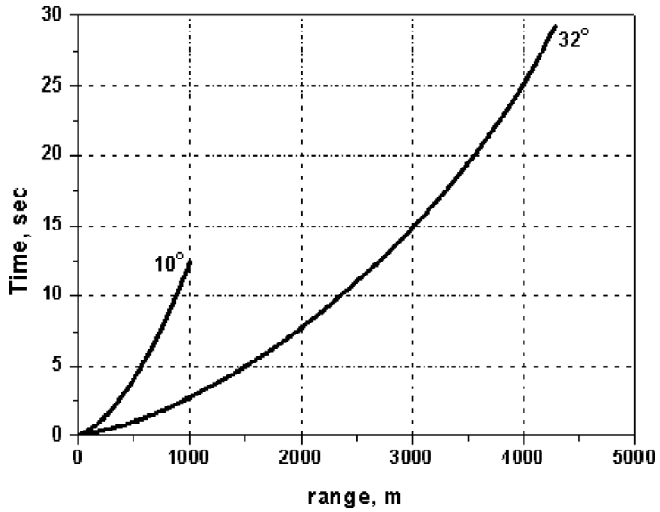

Figure 11: Flight Time Variations for 7.62 mm Bullet at Pitch Angles of 10° and 32°

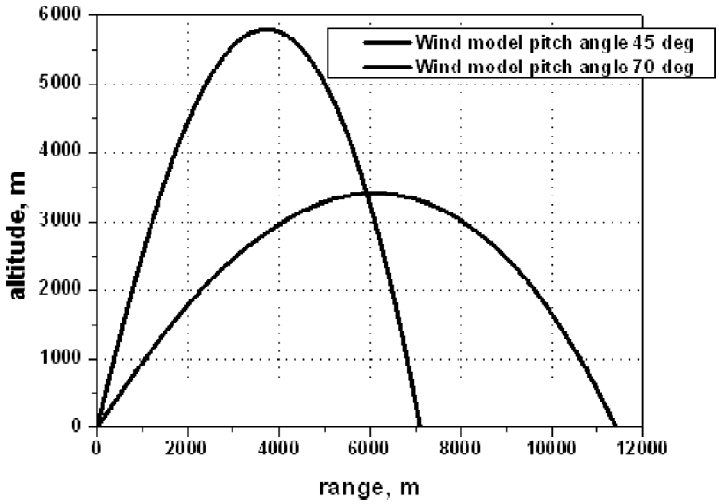

Figure 12: Wind Model Path Trajectories at Elevation Angles of 45° and 70° for 105 mm Projectile

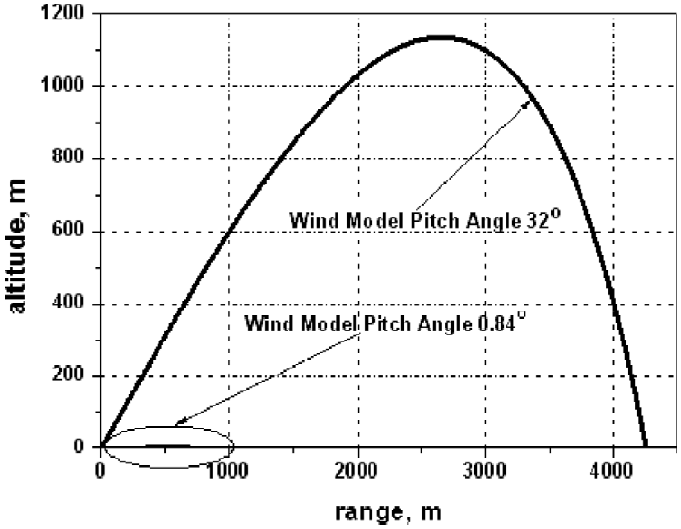

Figure 13: Wind Effects on 7.62 mm Bullet Trajectory Motion at Pitch Angles of 0.84° and 32°

Comparative computed trajectories of the 105 mm projectile at pitch angles of 45° and 70° with a 10.0 m/s mean crosswind blowing are indicated in Fig. 12. From the computational results of the applied method at 45°, the predicted range to impact (black solid line) is almost 11,400 m and the maximum height is slightly over 3,400 m. In addition, the predicted level-ground range (red solid line) at 70° for the crosswind trajectory estimation gives the corresponding values 7,100 m and 5,800 m, respectively.

Furthermore, Fig. 13 show the computational results for 7.62mm bullet at elevation angles of 0.84° and 32° with a 5.0 m/s mean crosswind effect. At 0.84° flat-fire trajectory, the range with the wind simulation model is almost 910 m (black solid line) and the maximum height 4.5 m. At 32° pitch angle, the wind predicted range to target impact area is 4,250 m (red solid line) and the height is almost 1,170 m.

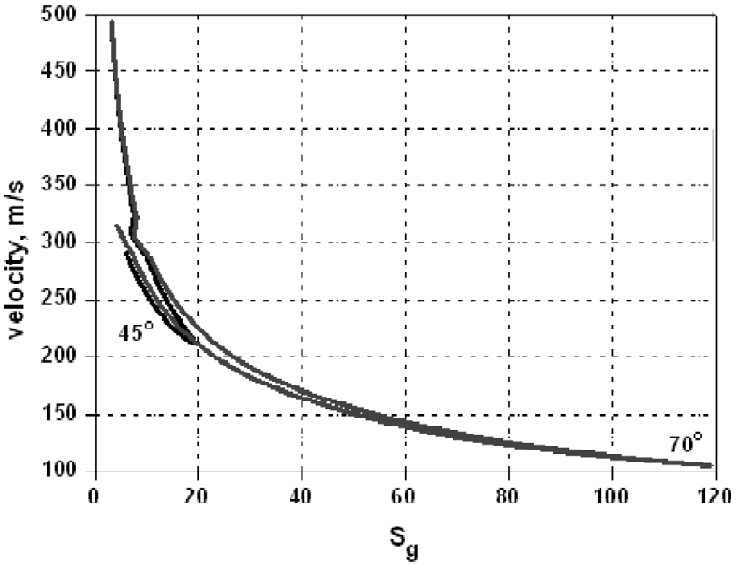

Figure 14: Comparative Static Stability Variations for 105 mm Projectile at High and Low Quadrant Angles

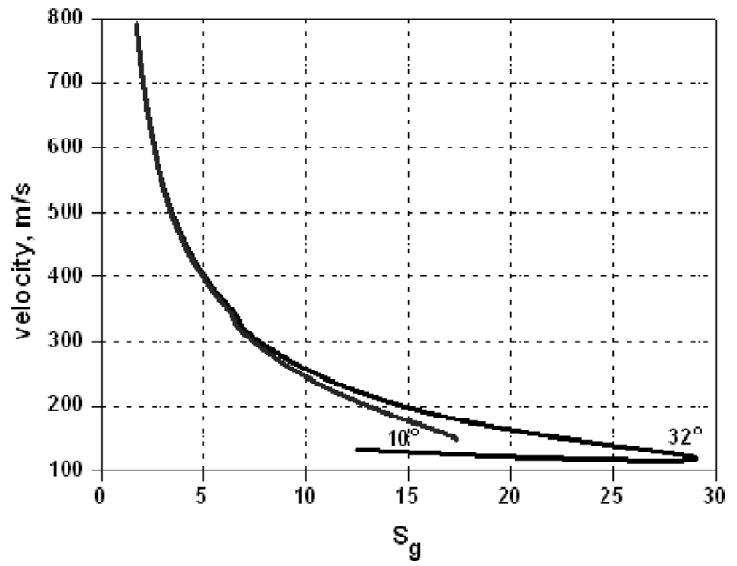

Figure 15: Static Stability Versus Velocity at Firing Pitch Angles of 10° and 32° for 7.62 mm Bullet

After the damping of the initial transient motion at apogee, the stability factor for 105mm projectile at 45° has increased from 3.1 at muzzle firing point to 19, when the value of velocity is 214 m/sec and then decreased to 6 with a velocity value of 291 m/sec at final impact point area, as presented in Fig. 14. The corresponding flight behavior at 70° initial pitch angle shows, that the gyroscopic static stability factor has increased from 3.1 to 121 where the velocity reaches the value of 100 m/sec. Then S_g decreases to 4.2 at the impact shooting point and the corresponding velocity value is 315 m/sec.

Figure 15 shows the static stability variations with range for 7.62 mm bullet, fired from a 12" twist per turn with a muzzle velocity of 793 m/s at quadrant elevation angles of 10° and 32°, respectively. The transient motion damps out very quickly for the two cases. The gyroscopic stability factor for 32° is 1.7 at muzzle, grows to 29 when the velocity value is almost 118 m/sec at the summit of the trajectory, and then the static factor decreases to a value of 12 and the velocity increases to 132 m/sec at the impact point. In addition, the stability factor for 10° initial firing angle was 1.7 at muzzle and then grows to value of 17 and decreases the velocity to the value 148 m/sec at the final target area.

8. CONCLUSION

The full six degrees of freedom (6-DOF) simulation flight dynamics model is applied for the accurate prediction of short and long range trajectories results for high and low spin-stabilized projectiles and small bullets. It takes into consideration the Mach number and the total angle of attack variation effects by means of the variable aerodynamic coefficients. The computational simulation of the applied variable flight model gives results of high accuracy in contrast to the corresponding analysis with constant aerodynamic coefficients.

Wind effects and static stability variations are also examined for 105mm big projectile and 7.62mm small bullet flight bodies at various initial firing conditions. The computational results of the proposed synthesized analysis are in good agreement compared with other technical data and recognized exterior atmospheric projectile flight computational models.

REFERENCES

[1] McCoy, R. (1999), *Modern Exterior Ballistics*, Schiffer, Attlen, PA, pp.165–183, 217–218, 244, 248.

[2] Fowler, R., Gallop, E., Lock, C., and Richmond H. (1920), "The Aerodynamics of Spinning Shell," *Philosophical Transactions of the Royal Society of London, Series A*: Mathematical and Physical Sciences, **221**.

[3] Cooper, G. (2001), "Influence of Yaw Cards on the Yaw Growth of Spin Stabilized Projectiles," *Journal of Aircraft,* **38**, 2.

[4] Guidos, B., and Cooper, G. (2000), "Closed Form Solution of Finned Projectile Motion Subjected to a Simple In-Flight Lateral Impulse," *AIAA Paper.*

[5] Costello, M., and Peterson, A. (2000), "Linear Theory of a Dual-Spin Projectile in Atmospheric Flight," *Journal of Guidance, Control, and Dynamics,* **23**, 5.

[6] Burchett, B., Peterson, A., and Costello, M. (2002), "Prediction of Swerving Motion of a Dual-Spin Projectile with Lateral Pulse Jets in Atmospheric Flight," *Mathematical and Computer Modeling,* **35**, 1-2, pp.1-14.

[7] Cooper, G. (2004), "Extending the Jump Analysis for Aerodynamic Asymmetry," *Army Research Laboratory*, ARL-TR-3265, pp.1-4.

[8] Cooper, G. (2003), "Projectile Aerodynamic Jump Due to Lateral Impulsives," *Army Research Laboratory*, ARL-TR-3087, pp.1-4.

[9] Murphy, C. (1981), "Instability of Controlled Projectiles in Ascending or Descending Flight," *Journal of Guidance, Control, and Dynamics,* **4**, 1.

[10] Hainz, L., and Costello, M. (2005), "Modified Projectile Linear Theory for Rapid Trajectory Prediction," *Journal of Guidance, Control, and Dynamics,* **28**, 5, pp.1007–1009.

[11] Etkin, B. (1972), *Dynamics of Atmospheric Flight,* John Wiley and Sons, New York.

[12] Joseph K., Costello, M., and Jubaraj S. (2006), "Generating an Aerodynamic Model for Projectile Flight Simulation Using Unsteady Time Accurate Computational Fluid Dynamic Results," *Army Research Laboratory,* ARL-CR-577, pp. 1-6.

[13] Amoruso, M. J. (1996), "Euler Angles and Quaternions in Six Degree of Freedom Simulations of Projectiles," Technical Note.

[14] Costello, M., and Anderson, D. (1996), "Effect of Internal Mass Unbalance on the Terminal Accuracy and Stability of a projectile," *AIAA Paper*

[15] Gkritzapis, D., N., Panagiotopoulos, E. E., Margaris, D. P., Papanikas, D. G. (2007): *"Atmospheric Flight Dynamic Simulation Modelling of Spin-Stabilized Projectiles"*, Proceedings of the 2nd International Conference on Experiments / Process / System Modelling / Simulation / Optimization, 2nd IC-EpsMsO, 4-7 July, Athens, Greece

[16] Nennstiel, R. (1996), "How do the Bullets Flight?" *Journal of AFTE*, **28**, No. 2.

Dimitrios N. Gkritzapis
Laboratory of Firearms and Tool Marks Section
Criminal Investigation Division, Captain of Hellenic Police
Hellenic Police, 11522, Athens Greece

or

Postgraduate Student of Fluid Mechanics Laboratory
University of Patras, 26500
Patras, Greece

Elias E. Panagiotopoulos
Postgraduate Student

Dionissios P. Margaris
Assistant Professor

Dimitrios G. Papanikas
Ex-Professor of Mechanical Engineering and Aeronautics Dept.
University of Patras, 26500, Patras, Greece